Low-Complexity Hybrid Transceivers for Uplink Multiuser mmWave MIMO by User Clustering

Darian Pérez-Adán, José P. González-Coma, Óscar Fresnedo and Luis Castedo
CITIC, Department of Computer Engineering, University of A Coruña, Spain
Email: {d.adan, jose.gcoma, oscar.fresnedo, luis}@udc.es

***Abstract*—The high cost and power consumption of millimeter wave (mmWave) radio frequency (RF) hardware elements demands for advanced signal processing techniques to design MIMO transceivers. Hybrid analog-digital architectures for MIMO transceivers have become an attractive strategy to reduce the number of RF chains of the transceivers. In the uplink of a multiuser mmWave MIMO system, this hardware reduction is limited by the number of users to be handled, which can be rather large. In this work, we propose to use distributed quantizer linear coding (DQLC) in order to superimpose correlated sources in a cluster-based uplink multiuser mmWave MIMO system and reduce the number of RF chains at the receiver. The scheduling policy to cluster the transmitters is also analyzed by considering the correlation of the sources and channel state information (CSI). Numerical results show the advantage of employing the proposed scheme to reduce hardware complexity.**

***Index Terms*—Millimeter wave, joint source-channel coding, uplink, source correlation, multiuser.**

I. Introduction

Millimeter wave (mmWave) bands are promising to achieve the high data rate demands of future wireless communication systems. However, mmWave wireless transmissions suffer from huge path losses. These can be compensated with high beamforming gains obtained with large antenna arrays (massive MIMO) physically viable due to the small wavelength. In conventional MIMO, there is usually a complete radio frequency (RF) chain per antenna, and transceiver operations are usually implemented at baseband. However, these fully digital implementations are prohibitive in massive MIMO mmWave due to the extremely high cost and power consumption of the RF hardware [1].

Hybrid analog-digital MIMO transceiver architectures have been considered to reduce the number of RF chains, N_{RF} [2], [3]. Two hybrid strategies have been explored: fully-connected structures (FCS) [2], where there is a full connection between all antennas and each RF chain and the structure based on subarrays [3] also called partially-connected structure (PCS), where each RF chains is connected to some antennas. In general, hybrid MIMO transceiver architectures present the constraint that N_{RF} cannot be smaller than the number of data streams, K. Consequently, most works focus on those cases where $K \leq N_{\mathrm{RF}} < 2K$ since the FCS hybrid precoding has been shown to achieve the performance of the fully digital precoder for $N_{\mathrm{RF}} \geq 2K$ [4].

In many applications (e.g., vehicular communications, wireless sensor networks, or IoT systems) the uplink of multiuser mmWave MIMO systems often involves a large number of individual users transmitting to a centralized receiver. Consequently, a high number of receive chains, $N_{\mathrm{RF}}^{\mathrm{r}}$, are necessary to properly receive all individual streams. In this work, we seek to reduce the number of receive RF chains, $N_{\mathrm{RF}}^{\mathrm{r}}$, in the uplink of a multiuser mmWave MIMO system by overlaying streams of analog correlated sources. We show that with $N_{\mathrm{RF}}^{\mathrm{r}} \leq K$ in FCS it is possible to obtain a reasonable system performance by clustering users through DQLC mapping. This mapping also offers the advantage of preserving the spectral efficiency of the system by establishing a zero-delay encoding. This proposed design is based on the well-known strategy of using a non-orthogonal multiple access scheme [5], [6].

A. Notation

We use the following notation: a represents a scalar and $\mathbf{a}$ is a vector, $\mathbf{A}_{i,j}$ is the entry on the i-th row and the j-th column of the matrix $\mathbf{A}$, $\mathbf{A}_{(i,:)}$ is the i-th row of $\mathbf{A}$. $\mathbf{A}_{(\overline{i:n},:)}$ is the resulting matrix after removing from the i-th to the n-th row of $\mathbf{A}$ and reshape $\mathbf{A} \in \mathbb{C}^{\mathrm{I}\times\mathrm{J}}$ to $\mathbf{A} \in \mathbb{C}^{(\mathrm{I}\text{-}\mathrm{N})\times\mathrm{J}}$. Null $(\cdot)$ is the operator that constructs an orthonormal basis for the null space of the input matrix. Transpose and conjugate transpose of $\mathbf{A}$ are denoted by $\mathbf{A}^T$ and $\mathbf{A}^*$, respectively; $\|\mathbf{A}\|_F$ denotes the Frobenius norm of $\mathbf{A}$ and blkdiag $(\cdot)$ stands for the operator that constructs a block diagonal matrix from input matrices. $\lfloor\cdot\rceil$ represents rounding operation. Expectation is denoted by $\mathbb{E}[\cdot]$.

II. System Model

Fig. 1 shows the uplink of a multiuser mmWave system where the K users are clustered in L groups of U users, i.e., $K = LU$. We assume that each user is equipped with N_{t} antennas and sends a single-stream of encoded symbols to the receiver. We also consider that the discrete-time continuous-amplitude symbols are correlated and follow a multivariate complex valued distribution with zero mean and covariance matrix $\mathbf{C}_{\mathrm{s}} = \mathbb{E}[\mathbf{s}\mathbf{s}^*]$, such that $[\mathbf{C}_{\mathrm{s}}]_{k,k} = 1 \ \forall k$ and $[\mathbf{C}_{\mathrm{s}}]_{i,j} = \rho_{i,j}$, $0 \leq \rho_{i,j} \leq 1 \ \forall i,j$ with $i \neq j$. Each user sends one complex-valued encoded symbol $f_{l,u}(s_{l,u})$ per channel use. Therefore, the vector corresponding to all encoded user symbols per channel use is given by $\mathbf{f}(\mathbf{s}) = [f_{1,1}(s_{1,1}), ..., f_{1,U}(s_{1,U}), f_{2,1}(s_{2,1}), ..., f_{L,U}(s_{L,U})]^T$, where $f_{l,u}(\cdot)$ represents the superposition function applied to the u-th user in the l-th cluster. We assume the encoded symbols are power normalized such that $\mathbb{E}[| \ f_{l,u}\left(s_{l,u}\right) |^2] \leq 1$.

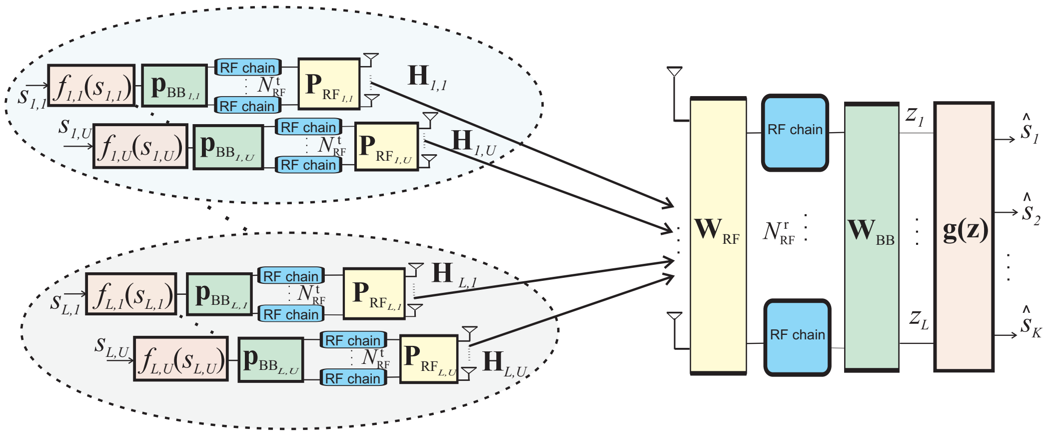

Fig. 1. Block diagram of the multiuser mmWave MIMO system with L clusters and U users per cluster.

Hybrid precoding is considered at the users. The hybrid precoder of the u-th user in the l-th cluster is $\mathbf{p}_{\mathrm{H}l,u} = \mathbf{P}_{\mathrm{RF}l,u}\mathbf{p}_{\mathrm{BB}l,u}$, which is implemented using $N_{\mathrm{RF}}^{\mathrm{t}}$ transmit chains. The baseband precoder is $\mathbf{p}_{\mathrm{BB}l,u} \in \mathbb{C}^{N_{\mathrm{RF}}^{\mathrm{t}}\times 1}$ and the analog precoder is $\mathbf{P}_{\mathrm{RF}l,u} \in \mathcal{P}_{\mathrm{RF}}{}^{N_{\mathrm{t}}\times N_{\mathrm{RF}}^{\mathrm{t}}}$ such that $\mathcal{P}_{\mathrm{RF}} \subset \mathbb{C}^{N_{\mathrm{t}}\times N_{\mathrm{RF}}^{\mathrm{t}}}$ is the set of feasible precoders with unit modulus entries [2], [3]. An individual power constraint is imposed at each user such that $\|\mathbf{P}_{\mathrm{RF}l,u}\mathbf{p}_{\mathrm{BB}l,u}\|_F^2 \leq T_{l,u}\ \forall l,u$.

At the receiver, the K data streams are collected by N_r antennas. The received signal can be expressed as

$$\mathbf{y} = \sum_{l=1}^{L}\sum_{u=1}^{U}\mathbf{H}_{l,u}\mathbf{P}_{\mathrm{RF}l,u}\mathbf{p}_{\mathrm{BB}l,u}f_{l,u}(s_{l,u}) + \mathbf{n}, \tag{1}$$

where $\mathbf{H}_{l,u} \in \mathbb{C}^{N_{\mathrm{r}}\times N_{\mathrm{t}}}$ represents the mmWave channel response of the u-th user in the l-th cluster of users and $\mathbf{n} = [n_1, n_2, ..., n_{N_{\mathrm{r}}}]^T$ is the complex-valued additive white Gaussian noise (AWGN) such that $\mathbf{n} \sim \mathcal{N}_{\mathbb{C}}(0, \sigma_{\mathrm{n}}^2\mathbf{I})$. The received signal in (1) can be rewritten as

$$\mathbf{y} = \mathbf{H}\mathbf{P}_{\mathrm{H}}\mathbf{f}(\mathbf{s}) + \mathbf{n}, \tag{2}$$

by using horizontal concatenation for the channel responses $\mathbf{H} = [\mathbf{H}_{1,1}\cdots\mathbf{H}_{L,U}]$, and the matrix containing all the hybrid precoders $\mathbf{P}_{\mathrm{H}} = \mathrm{blkdiag}\left(\mathbf{p}_{\mathrm{H}1,1}, ..., \mathbf{p}_{\mathrm{H}L,U}\right)$. We assume $N_{\mathrm{RF}}^{\mathrm{r}}$ is strictly limited by $N_{\mathrm{RF}}^{\mathrm{r}} < K$, The channel responses are also assumed to be perfectly known at both ends.

A. Channel Model

We assume a clustered channel model which is a fairly accurate mathematical representation of the mmWave channel [7]. The channel is composed by N_{cl} scattering clusters, and each cluster contains N_{ray} rays [7], [8]. Therefore, the narrowband MIMO channel model is described by

$$\mathbf{H}_{l,u} = \gamma\sum_{i=1}^{N_{\mathrm{cl}}}\sum_{m=1}^{N_{\mathrm{ray}}}\beta_{i,m}\mathbf{a}_{\mathrm{r}}(\phi_{i,m}^{\mathrm{r}}, \theta_{i,m}^{\mathrm{r}})\mathbf{a}_{\mathrm{t}}^{*}(\phi_{i,m}^{\mathrm{t}}, \theta_{i,m}^{\mathrm{t}}), \tag{3}$$

where $\gamma = \sqrt{N_{\mathrm{t}}N_{\mathrm{r}}/N_{\mathrm{cl}}N_{\mathrm{ray}}}$ represents a normalization factor, $\beta_{i,m}$ is the complex gain of the m-th ray in the i-th scattering cluster. $\phi^{\mathrm{t}}(\theta^{\mathrm{t}})$ and $\phi^{\mathrm{r}}(\theta^{\mathrm{r}})$ are the azimuth (elevation) angles of departure (AoDs) and arrival (AoAs), respectively. The transmit and receive steering vectors are represented by $\mathbf{a}_{\mathrm{t}}(\phi^{\mathrm{t}}, \theta^{\mathrm{t}})$ and $\mathbf{a}_{\mathrm{r}}(\phi^{\mathrm{r}}, \theta^{\mathrm{r}})$. We consider uniform square planar array (USPA) of $\sqrt{N}\times\sqrt{N}$ antennas at both ends, hence, the steering vectors are computed as

$$\begin{aligned}\mathbf{a}(\phi,\theta) = &\frac{1}{\sqrt{N}}\Big[1, ..., e^{j\frac{2\pi}{\lambda}d(p\,\sin(\phi)\,\sin(\theta)+q\,\cos(\theta))},\\ &..., e^{j\frac{2\pi}{\lambda}d\left(\left(\sqrt{N}-1\right)\sin(\phi)\sin(\theta)+\left(\sqrt{N}-1\right)\cos(\theta)\right)}\Big]^T,\end{aligned} \tag{4}$$

where λ and d represent the wavelength and the antenna spacing, respectively. We use the indices $0 \leq p < \sqrt{N}$ and $0 \leq q < \sqrt{N}$ to indicate the position of the array elements.

III. User Clustering in mmWave Hybrid Systems

Most works on hybrid MIMO transceivers focus on the cases $K \leq N_{\mathrm{RF}}^{\mathrm{r}} < 2K$. However, in the uplink of a multiuser mmWave MIMO system, the number of users K simultaneously served by the same receiver could be large. In order to reduce $N_{\mathrm{RF}}^{\mathrm{r}}$ down to $L = K/U$, we group the K users into L clusters so that the U users at each cluster use a DQLC mapping to encode their source symbols. This mapping strategy is designed to ensure that the receiver is able to recover the U user symbols from the superimposed symbol resulting from their sum, being L the number of individual streams produced after the overlapping. Note that the use of DQLC allows reducing the number of RF chains required at reception without lowering the spectral efficiency. In addition, this encoding strategy presents some additional advantages such as a negligible delay and efficient exploitation of the source correlation.

A. DQLC Mapping

DQLC is a joint source-channel coding method proposed for analog transmission of distributed Gaussian sources over the multiple access channel (MAC) [9]. This mapping represents a special case of vector quantizer linear coding (VQLC) for zero-delay scenarios [10]. In DQLC, $U-1$ users of the group send a quantized version of its symbol while the symbol of the remaining user is scaled by a factor. Hence, the DQLC mapping function for the l-th cluster is given by

$$f_{l,u}\left(s_{l,u}\right)=\begin{cases}\alpha_{l,u}\left\lfloor\frac{s_{l,u}}{\Delta_{l,u}}-\frac{1}{2}\right\rceil+\frac{1}{2}, & 1\leq u\leq U-1\\ \alpha_{l,u}s_{l,u}, & u=U\end{cases}, \quad (5)$$

where $\alpha_{l,u}$ is a gain factor and $\Delta_{l,u}$ represents the quantization step of the quantizer used for the u-th user in the l-th cluster. Note that L individual channel symbols will produce all the estimated user symbols ($K = LU$) by demapping each channel symbol into U estimated user symbols through DQLC decoding functions.

B. Demapping

The signal after a hybrid linear filter at the receiver, $\mathbf{W}_{\mathrm{H}} = \mathbf{W}_{\mathrm{RF}}\mathbf{W}_{\mathrm{BB}}$, is expressed as

$$\mathbf{z}=\mathbf{W}_{\mathrm{BB}}^{*}\mathbf{W}_{\mathrm{RF}}^{*}\mathbf{y}, \quad (6)$$

where $\mathbf{W}_{\mathrm{BB}}^{*}\in\mathbb{C}^{L\times N_{\mathrm{RF}}^{\mathrm{r}}}$ and $\mathbf{W}_{\mathrm{RF}}^{*}\in\mathcal{W}_{\mathrm{RF}}^{*}$ denote the baseband combiner and the RF combiner respectively. $\mathcal{W}_{\mathrm{RF}}^{*}\subset\mathbb{C}^{N_{\mathrm{RF}}^{\mathrm{r}}\times N_{\mathrm{r}}}$ represents the set of feasible RF combiners with constant-magnitude entries. Note that the combiner actually provides L channel symbol streams, which enables low-complexity schemes with $N_{\mathrm{RF}}^{\mathrm{r}} = L$. Then, the estimated symbols $\hat{\mathbf{s}}=[\hat{s}_{1,1},...,\hat{s}_{L,U}]^T$ are produced by the decoding functions $\mathbf{g}(\mathbf{z})=[g_1(z_1),...,g_L(z_L)]$.

The optimization of DQLC mapping parameters is the key to recover the source symbols of the users of the l-th cluster from the l-th symbols provided by the combiner. This optimization has been discussed in [11, Section IV], here we follow the same approach by considering the total equivalent channel

$$\mathbf{H}_{\mathrm{v}}=\mathbf{W}_{\mathrm{H}}^{*}\mathbf{H}\mathbf{P}_{\mathrm{H}}. \quad (7)$$

Different algorithms have been developed for DQLC demapping such as sequential decoding [10, Section III], where an estimation of the quantized symbols is made, and these estimated symbols are then used to estimate the scaled symbol. Another decoding strategy is the approximated minimum mean squared error (MMSE) estimation using sphere decoding [11, Section III], which presents a better performance for more than two users per cluster by considering the posterior probability. Hence, we use this decoding algorithm since it can also be applied for an arbitrary number of users (see [11] for details).

C. Scheduling for User Clustering

In this section, the user clustering allocation by considering the correlation and the CSI is addressed. For the sake of fairness, we assume the same power constraint per user i.e., $T_{l,u} = T$, $\forall l, u$ and the same number of users per cluster.

From [11], [12] it is clear the improvement of DQLC mapping performance by exploiting spatial correlation. Hence, we group the users into the different clusters following a strategy based on the user correlation. A key point in the DQLC performance is to avoid the anomalous distortion given by the erroneous detection of any quantized symbol [9] because, when quantization levels are interchanged, the detection of the scaled symbol will be also erroneous. Hence, we assume that the quantized version of the DQLC mapping corresponds to the users in the cluster, whose channel matrices have larger singular values. In summary, the scheduling policy is established as follows:

(i) The users with higher cross-correlation factor would be in the same cluster.
(ii) The users into the l-th cluster whose channel matrices have larger singular values use the quantized version of the DQLC mapping and the remaining user establishes the scaled version.

Note that user cooperation is not necessary since the allocation is performed by the receiver.

D. Unconstrained Precoding and Combining

Unconstrained overall digital precoding design in MIMO systems has been explored in several works. Among the several precoding strategies considered in [13], we choose the Nu-SVD unconstrained precoding strategy [13, Section III] since we need to cancel the inter-cluster interference. Hence, the unconstrained digital filter at the receiver, $\mathbf{W}^{*}\in\mathbb{C}^{L\times N_{\mathrm{r}}}$, is designed to satisfy the following condition

$$\mathbf{W}_{(j,:)}^{*}\mathbf{H}_{l,u}\mathbf{P}_{\mathrm{RF}l,u}\mathbf{p}_{\mathrm{BB}l,u}=0\ \forall l,u\ \ \text{s.t}\ \ j\neq l\ , \quad (8)$$

i.e., the j-th row of the filter is into the null space of the conjugate transpose of the matrix given by the equivalent channels $\tilde{\mathbf{h}}_{l,u}=\mathbf{H}_{l,u}\mathbf{P}_{\mathrm{RF}l,u}\mathbf{p}_{\mathrm{BB}l,u}$ corresponding to the remaining clusters of users. Hence, each row is chosen as the vector into the null space that maximizes the signal-to-noise ratio (SNR) as

$$\mathbf{W}_{(l,:)}^{*}=\left(\mathbf{N}_l\mathbf{N}_l^{*}\left(\tilde{\mathbf{h}}_{l,1}+...+\tilde{\mathbf{h}}_{l,U}\right)\right)^{*}, \quad (9)$$

where $\mathbf{N}_l$ is an orthonormal basis for the null space of the conjugate transpose of the matrix given by the equivalent channels corresponding to the remaining clusters of users, i.e.,

$$\mathbf{N}_l=\text{Null}\left(\tilde{\mathbf{H}}_{\overline{((l-1)U+1\,:\,lU,\,:\,)}}^{*}\right),\quad l=1,...,L\ , \quad (10)$$

where $\tilde{\mathbf{H}}=[\tilde{\mathbf{h}}_{1,1}\cdots\tilde{\mathbf{h}}_{L,U}]$. Then, at the output of the combiner $\mathbf{W}^{*}$, we have the received signal decoupled as

$$\mathbf{z}=\Big[\mathbf{W}_{(1,:)}^{*}\left(\tilde{\mathbf{h}}_{1,1}f_{1,1}(s_{1,1})+...+\tilde{\mathbf{h}}_{1,U}f_{1,U}(s_{1,U})+\mathbf{n}\right), \\ ...,\mathbf{W}_{(L,:)}^{*}\left(\tilde{\mathbf{h}}_{L,1}f_{L,1}(s_{L,1})+...+\tilde{\mathbf{h}}_{L,U}f_{L,U}(s_{L,U})+\mathbf{n}\right)\Big]^{T}. \quad (11)$$

Each element z_l of the vector $\mathbf{z}\in\mathbb{C}^{L\times 1}$ contains all the summed U symbols from the l-th user cluster.

E. Precoding and Combining with Limited RF Chains

We assume each user performs hybrid precoding with $N_{\mathrm{RF}}^{\mathrm{t}} = 2$. This amount of RF chains per user is enough to achieve essentially the same performance as that reached with the unconstrained precoder [4]. For the case of hybrid combining at reception, we consider two possibilities. When $N_{\mathrm{RF}}^{\mathrm{r}}\geq 2L$, we use the closed-form expression in [4] achieving the same performance as the digital combiner. For $L \leq N_{\text{RF}}^{\text{r}} < 2L$, the PG algorithm from [2] is employed to factorize the digital combiner into the baseband and RF components.

IV. Simulation Results

In this section, we provide numerical results of the performance of the proposed solution. The covariance matrix of the source symbols is assumed to be Toeplitz such that $[\mathbf{C}_{\text{s}}]_{i,j} = \rho^{|i-j|}\ \forall i,j$. In this correlation model, the probability of having uncorrelated sources increases with the number of users, K. We assume $N_{\text{t}} = 16$ and $N_{\text{r}} = 100$. The maximum and minimum number of clusters and rays per user is set to $N_{\text{cl}_{\text{max}}} = 8$, $N_{\text{ray}_{\text{max}}} = 16$ and $N_{\text{cl}_{\text{min}}} = 2$, $N_{\text{ray}_{\text{min}}} = 4$, respectively. Then, channel responses are modeled randomly as $N_{\text{cl}l,u} \in \{N_{\text{cl}_{\text{min}}}, ..., N_{\text{cl}_{\text{max}}}\}$ clusters with $N_{\text{ray}_{l,u}} \in \{N_{\text{ray}_{\text{min}}}, ..., N_{\text{ray}_{\text{max}}}\}$. The path gain $\beta_{i,m}$ is assumed to be a random variable following the complex Gaussian distribution $\mathcal{CN}(0,1)$. The angles of departure and arrival (AoA/AoD) are normal randomly distributed with mean angle uniformly randomly distributed in $[0, 2\pi)$ and the angular spread is 8 degrees. Finally, all the reported results are averaged over $N = 1000$ random channel realizations. Performance is assessed in terms of the signal-to-distortion ratio (SDR) defined as SDR (dB) $= 10 \log_{10}\left(\frac{1}{\hat{\xi}_{\text{sum}}}\right)$ where

$$\hat{\xi}_{\text{sum}} = \frac{1}{NLU}\sum_{n=1}^{N}\sum_{l=1}^{L}\sum_{u=1}^{U}|s_{n,l,u} - \hat{s}_{n,l,u}|^2. \tag{12}$$

The SDR parameter is plotted versus the SNR. We assume $\sigma_{\text{n}}^2 = 1$. Hence, the SNR per user is $\text{SNR (dB)}_{l,u} = 10 \log_{10}(T_{l,u})\ \forall l,u$.

We present the results of three experiments in order to analyze the impact of the scheduling policy choice, the system behavior when the number of users increases, and the performance of DQLC mappings.

In the first experiment, we compare the obtained performance with the proposed scheduling policy and a random scheduling policy where the user clustering and the DQLC allocation are random. Results are shown for two different correlation factors, $\rho = 0.6$ and $\rho = 0.2$, and two different numbers of receive RF chains, $N_{\text{RF}}^{\text{r}} = 6$ and $N_{\text{RF}}^{\text{r}} = 8$. $K = 12$ users are assumed and the number of users per cluster is chosen according to the hardware constraint: $U = 3$ for $N_{\text{RF}}^{\text{r}} = 8$ and $U = 4$ for $N_{\text{RF}}^{\text{r}} = 6$. Therefore, we can use the closed-form expression from [4] for the factorization. Fig. 2 shows that the proposed scheduling policy provides a significant performance gain with respect to the random strategy. As expected, this gain increases as the correlation become higher. From this figure, it is clear that the system performance is lower when the hardware constraint is higher and more users per group are included. Nevertheless, a reasonable performance is obtained even in the lower hardware complexity case ($N_{\text{RF}}^{\text{r}} = 6$).

We now evaluate the performance gain of the proposed scheduling policy by increasing the number of users K. The gain is defined as $G\ \text{(dB)} = \text{SDR}_{\text{sc}}(\text{dB}) - \text{SDR}_{\text{rm}}(\text{dB})$,

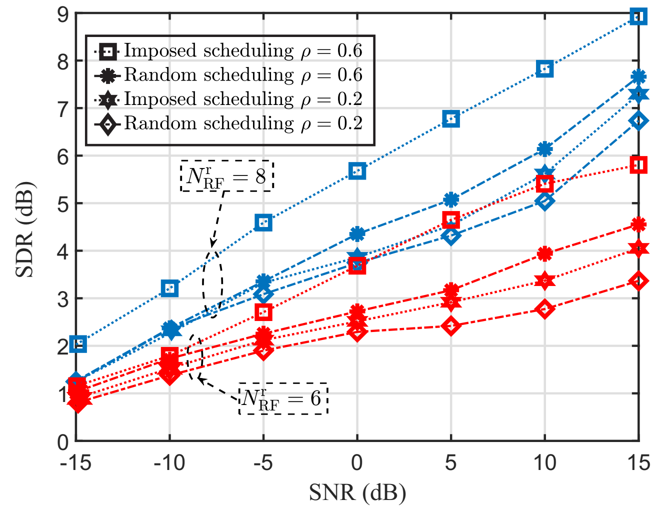

Fig. 2. SDR (dB) performance for $K = 12$ users, $N_{\text{RF}}^{\text{r}} \in \{6, 8\}$, $U \in \{3, 4\}$ and different correlation factors $\rho \in \{0.2, 0.6\}$.

where $\text{SDR}_{\text{sc}}(\text{dB})$ and $\text{SDR}_{\text{rm}}(\text{dB})$ represent the SDR with the proposed scheduling policy and the random scheduling policy, respectively. Fig. 3 shows the performance gains obtained for typical SNR values in mmWave as the number of users increases. As expected, the performance gain due to the proposed scheduling increases with the number of users. In that case, the performance of the random scheduling will be worse since the probability of clustering low-correlated users is higher. Furthermore, the choice of the users for DQLC allocation according to the CSI represents a key point for the behavior of DQLC mapping. Note that the performance gain saturates for a high number of users depending on the correlation. This is as a consequence of the larger number of uncorrelated sources, which establishes that the system performance with a random clustering approaches that with uncorrelated sources.

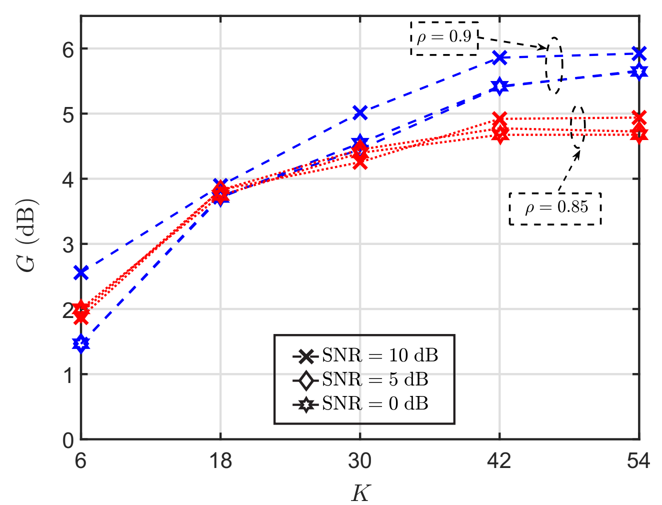

Fig. 3. Behavior of the performance gain (dB) of the proposed scheduling policy according the number of users for different correlation factors $\rho \in \{0.85, 0.90\}$, $U = 3$ users per cluster and SNR (dB) $\in \{0, 5, 10\}$.

In the last experiment, we compare the performance of the proposed scheme to that of a non-orthogonal linear transmission using the same clustering approach. In this scheme, the precoders are designed to align the users into the group to the best receiver direction. Then, the linear filter $\mathbf{W}^*$ in (9) is used to decouple the received signal and an MMSE detection produces the estimated symbols. This simulation is helpful to evaluate the behavior of DQLC mapping for superposition. Fig. 4 shows the SDR achieved by considering

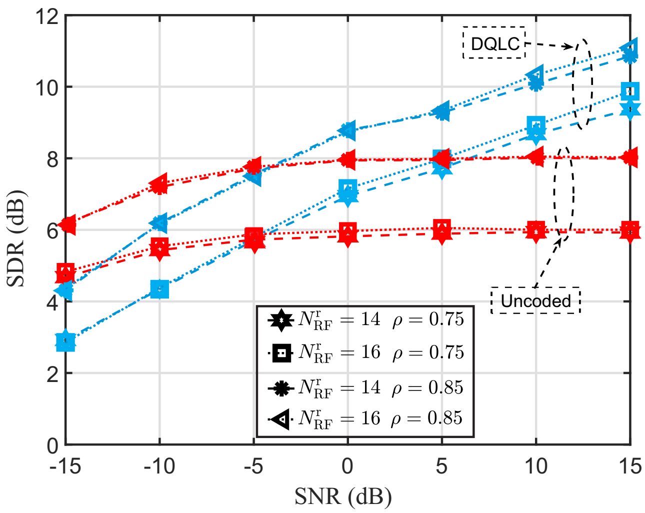

Fig. 4. SDR (dB) performance by implementing user clustering with $K = 24$ users, $U = 3$ users per cluster, $N_{\text{RF}}^{\text{r}} \in \{14, 16\}$ receive chains and different correlation factors $\rho \in \{0.75, 0.85\}$.

$N_{\text{RF}}^{\text{r}} \in \{14, 16\}$, $K = 24$ and $U = 3$. Results are obtained by considering user clustering for encoded and uncoded scenarios assuming the proposed clustering policy regarding the correlation. For the encoded solution, the assumed DQLC allocation depending on the CSI is also considered. The PG algorithm is considered to solve the matrix factorization for $L \leq N_{\text{RF}}^{\text{r}} < 2L$ and the closed-form expression from [4] for $N_{\text{RF}}^{\text{r}} = 2L$. It is shown that for low SNRs, the performance of the uncoded scheme is higher, but its performance saturates above some SNR value depending on the correlation. The gap in the graphs for different numbers of RF chains is given by the error of the PG matrix factorization algorithm for the case of $N_{\text{RF}}^{\text{r}} = 14$, since for $N_{\text{RF}}^{\text{r}} = 16$ the factorization is perfect.

V. Conclusion

In this paper, we have addressed the use of user clustering with DQLC mapping for the uplink of multiuser mmWave MIMO systems with limited RF chains. A scheduling policy based on the source correlation and the CSI has been proposed in order to maximize the system performance. Results show that the proposed scheduling policy provides reasonable gains compared to a random scheduling policy to cluster the users. Furthermore, a low-complexity solution to the uplink of multiuser mmWave MIMO systems for a large number of analog correlated sources has also been proposed.

Acknowledgments

This work has been funded by the Xunta de Galicia (ED431C 2016-045, ED431G/01), the Agencia Estatal de Investigación of Spain (TEC2016-75067-C4-1-R) and ERDF funds of the EU (AEI/FEDER, UE), and the predoctoral grant BES-2017-081955.

References

[1] R. W. Heath, N. Gonzalez-Prelcic, S. Rangan, W. Roh, and A. M. Sayeed, "An Overview of Signal Processing Techniques for Millimeter Wave MIMO Systems," *IEEE Journal of Selected Topics in Signal Processing*, vol. 10, no. 3, pp. 436–453, Apr. 2016.

[2] J. P. Gonzalez-Coma, J. Rodriguez-Fernandez, N. Gonzalez-Prelcic, L. Castedo, and R. W. Heath, "Channel Estimation and Hybrid Precoding for Frequency Selective Multiuser mmWave MIMO Systems," *IEEE Journal of Selected Topics in Signal Processing*, vol. 12, no. 2, pp. 353–367, May 2018.

[3] N. Li, Z. Wei, H. Yang, X. Zhang, and D. Yang, "Hybrid Precoding for mmWave Massive MIMO Systems With Partially Connected Structure," *IEEE Access*, vol. 5, pp. 15 142–15 151, 2017.

[4] Xinying Zhang, A. Molisch, and Sun-Yuan Kung, "Variable-phase-shift-based RF-baseband codesign for MIMO antenna selection," *IEEE Transactions on Signal Processing*, vol. 53, no. 11, pp. 4091–4103, Nov. 2005.

[5] T. M. Cover and J. A. Thomas, *Elements of Information Theory*. New York: Wiley, 1991.

[6] S. Vanka, S. Srinivasa, Z. Gong, P. Vizi, K. Stamatiou, and M. Haenggi, "Superposition coding strategies: Design and experimental evaluation," *IEEE Transactions on Wireless Communications*, vol. 11, no. 7, pp. 2628–2639, 2012.

[7] A. Sayeed, "Deconstructing multiantenna fading channels," *IEEE Transactions on Signal Processing*, vol. 50, no. 10, pp. 2563–2579, Oct. 2002.

[8] L. Correia and P. Smulders, "Characterisation of propagation in 60 GHz radio channels," *Electronics & Communication Engineering Journal*, vol. 9, no. 2, pp. 73–80, Apr. 1997.

[9] P. A. Floor, A. N. Kim, T. A. Ramstad, I. Balasingham, N. Wernersson, and M. Skoglund, "On Joint Source-Channel Coding for a Multivariate Gaussian on a Gaussian MAC," *IEEE Transactions on Communications*, vol. 63, no. 5, pp. 1824–1836, May 2015.

[10] P. A. Floor, A. N. Kim, T. A. Ramstad, and I. Balasingham, "On transmission of multiple gaussian sources over a gaussian mac using a vqlc mapping," in *2012 IEEE Information Theory Workshop*. IEEE, 2012, pp. 50–54.

[11] P. Suárez-Casal, O. Fresnedo, and L. Castedo, "DQLC optimization for joint source channel coding of correlated sources over fading MAC," in *2018 26th European Signal Processing Conference (EUSIPCO)*, Sep. 2018, pp. 1292–1296.

[12] P. A. Floor, A. N. Kim, N. Wernersson, T. A. Ramstad, M. Skoglund, and I. Balasingham, "Zero-Delay Joint Source-Channel Coding for a Bivariate Gaussian on a Gaussian MAC," *IEEE Transactions on Communications*, vol. 60, no. 10, pp. 3091–3102, Oct. 2012.

[13] P. Suarez-Casal, J. P. Gonzalez-Coma, O. Fresnedo, and L. Castedo, "Design of Linear Precoders for Correlated Sources in MIMO Multiple Access Channels," *IEEE Transactions on Communications*, vol. 66, no. 12, pp. 6110–6122, Dec. 2018.